Vol. 44 — N° 3 09 20 P. 523 – 535

GEOSTANDARDS and GEOANALYTICAL RESEARCH

The $\delta^{60/58}$Ni Values of Twenty-Six Selected Geological Reference Materials

Weihan **Li** (1), Jian-Ming **Zhu** (1)*, Decan **Tan** (2, 3), Guilin **Han** (1), Zhouqiao **Zhao** (4) and Guangliang **Wu** (1)

(1) State Key Laboratory of Geological Processes and Mineral Resources, China University of Geosciences, Beijing 100083, China
(2) State Key Laboratory of Environmental Geochemistry, Institute of Geochemistry, Chinese Academy of Sciences, Guiyang 550081, China
(3) University of Chinese Academy of Sciences, Beijing 100049, China
(4) Department of Atmosphere and Ocean Sciences, School of Physics, Peking University, Beijing 100871, China
* Corresponding author. e-mail: jmzhu@cugb.edu.cn

The high-precision $\delta^{60/58}$Ni values of twenty-six geological reference materials, including igneous rocks, sedimentary rocks, stream sediments, soils and plants are reported. The $\delta^{60/58}$Ni values of all samples were determined by double-spike MC-ICP-MS (Nu Plasma III). Isotope standard solution (NIST SRM 986) and geological reference materials (BHVO-2, BCR-2, JP-1, PCC-1, etc.) were used to evaluate the measurement bias and intermediate precision over a period of six months. Our results show that the intermediate precision of Ni isotope determination was 0.05‰ (2*s*, *n* = 69) for spiked NIST SRM 986 and typically 0.06‰ for actual samples, and the $\delta^{60/58}$Ni $_{\text{NIST SRM 986}}$ values were in excellent agreement with previous studies. Eighteen high-precision Ni isotope ratios of geological reference materials are first reported here, and their $\delta^{60/58}$Ni values varied from -0.27‰ to 0.52‰, with a mean of 0.13 ± 0.34‰ (2*s*, *n* = 18). Additionally, SGR-1b (0.56 ± 0.04‰, 2*s*), GSS-1 (-0.27 ± 0.06‰, 2*s*), GSS-7 (-0.11 ± 0.01‰, 2*s*), GSD-10 (0.46 ± 0.06‰, 2*s*) and GSB-12 (0.52 ± 0.06‰, 2*s*) could potentially serve as candidate reference materials for Ni isotope fractionation and comparison of Ni isotopic compositions among different laboratories.

Keywords: nickel isotopes, $\delta^{60/58}$Ni, geological reference materials, double spike, MC-ICP-MS.

Received 24 Jul 19 – Accepted 16 Feb 20

Nickel (Ni) is a transition metal element located in group VIII and the fourth period of the Periodic Table. In the natural environment, Ni often exists in the II+ form. Nickel is mainly enriched in the Earth's core and mantle; the contents of Ni in core, lower and upper mantle are 5.35%, 0.19% and 0.2%, respectively (Javoy *et al.* 2010), while the mean mass fraction of Ni is 59 μg g^{-1} in the bulk continental crust (Rudnick and Gao 2003). In sedimentary environments, the ratio of trace elements Ni/Co and V/(V + Ni) is often used as a redox proxy to evaluate the depositional environment (Hatch and Leventhal 1992, Jones and Manning 1994, Schovsbo 2001).

As a bio-essential element, Ni plays a crucial role in the synthesis of methyl-coenzyme M reductase (MCR) for methanogens and urease for higher plants (Dixon *et al.* 1975, Hogan *et al.* 1983, Watt and Ludden 1999, Fraústo da Silva and Williams 2001, Ragsale 2007). Nickel is widely used in smelting, electroplating and other industries (Barnett 2010, Mudd 2010). In addition, nickel has attracted much attention in environmental protection and safety because of the toxicity of Ni tetracarbonyl ($(NiCO)_4$) (Shi 1994, Denkhaus and Salnikow 2002).

Nickel has five stable isotopes, namely ^{58}Ni (68.0769%), ^{60}Ni (26.2231‰), ^{61}Ni (1.1399%), ^{62}Ni (3.6345%) and ^{64}Ni (0.9256%) (Meija *et al.* 2016). Previous research on Ni isotopes mainly focused on meteorite and other extra-terrestrial samples. For instance, based on ^{60}Fe decaying to ^{60}Ni with a short half-life ($t_{1/2}$ = 2.62 My) (Rugel *et al.* 2009), the Ni isotope system has been used in cosmochemistry to trace the evolution of planets (Steele *et al.* 2012, Tang and Dauphas 2012, Elliott and Steele 2017, Render *et al.* 2018, Nanne *et al.* 2019). With the rapid development of multiple-collector inductively coupled plasma-mass spectrometry (MC-ICP-MS), high-precision Ni isotope ratios in terrestrial samples can be

doi: 10.1111/ggr.12321

determined easily and quickly. Earlier studies have indicated that the range of $\delta^{60/58}$Ni values reported from anthropogenic and natural sources is -1.03‰ to +2.5‰ (Cameron *et al.* 2009, Gall *et al.* 2013, Gueguen *et al.* 2013, Cameron and Vance 2014, Porter *et al.* 2014, Estrade *et al.* 2015, Ratié *et al.* 2015, Ventura *et al.* 2015, Ratié *et al.* 2016, Šillerová *et al.* 2017, Spivak-Birndorf *et al.* 2018). Nickel isotope fractionation mainly occurs in the process of biological utilisation and rock weathering in natural environments. The uptake and utilisation of Ni by methanogens and plants can result in large Ni isotope fractionation, up to 1.46‰ (Cameron *et al.* 2009, Deng *et al.* 2014). The Ni isotopic fractionation caused by rock weathering can reach 0.63‰ (Estrade *et al.* 2015, Ratié *et al.* 2015). Furthermore, chemical precipitation and adsorption can also produce different extents of Ni isotope fractionation (Gall *et al.* 2013, Wasylenki *et al.* 2014, 2015, Gueguen *et al.* 2016, 2018, Spivak-Birndorf *et al.* 2018). In recent years, Ni isotope ratios have gradually developed to be a new geochemical index and have been widely used to survey biogeochemical processes (Cameron *et al.* 2009, Deng *et al.* 2014), to investigate the onset of the Great Oxidation Event (GOE) (Konhauser *et al.* 2009, Wang *et al.* 2019) and to trace Ni pollution sources (Ratié *et al.* 2016, Šillerová *et al.* 2017).

Nevertheless, in order to evaluate and standardise geological data on Ni isotope ratios, geological reference materials (RMs) are still a prerequisite to further compare Ni isotope measurement results between different laboratories (Roelandts 1989, Okai *et al.* 2002, Jochum *et al.* 2005). Previous studies have identified Ni isotope ratios in some igneous reference materials such as peridotite (JP-1), basalt (BHVO-2, BCR-2), diabase (DNC-1), rhyolite (JR-2), andesite (AGV-2) and granite (G-2) (Cameron *et al.* 2009, Steele *et al.* 2011, Gueguen *et al.* 2013, Ratié *et al.* 2015, Chernonozhkin *et al.* 2015, Wu *et al.* 2019), while the sedimentary rock and soil reference materials are mainly limited to SGR-1, SCO-1, SDO-1 CLB-1 and NIST SRM 2711a (Gueguen *et al.* 2013, Ventura *et al.* 2015, Wang and Wasylenki 2017, Wu *et al.* 2019). As mentioned above, Ni isotope ratios have great potential for tracking sources and studying physiological processes. However, Ni isotope ratios in some common geological RMs with different characteristics, such as soils, stream sediments and plants, are still lacking. The limited availability of reference materials not only restricts interlaboratory comparisons of high-precision Ni isotope ratio measurement results but also restrains the feasibility in the evaluation of measurement procedures.

In this study, the Ni isotope ratios of twenty-six geological RMs were determined using double-spike MC-ICP-MS. These materials cover a wide range of compositions, including igneous rocks, sedimentary rocks, stream sediments, soils and plants (Table 1). Our work aims to enrich the Ni isotopes database in various geological reservoirs and to present reference values for interlaboratory comparison and quality control for various geological and environmental samples.

Experimental procedure

Reagents and materials

Optima-grade HNO_3, HCl and HF were obtained from the Beijing Institute of Chemical Reagents and further purified by Savillex's sub-boiling distiller (DST-4500). High purity water (HPW) with an 18.2 MΩ cm resistivity was prepared by a Milli-Q Element system (Burlington, MA, USA). Spectrum pure acetone, ACS-grade DMG and 35% *m/m* GR-grade H_2O_2 were purchased from Sinopharm Chemical Reagent Limited Corporation (Shanghai, China), Sigma-Aldrich (Shanghai, China) and Alfa Aesar (Tianjing, China), respectively. PFA beakers (15 ml capacity), pipette tips (5, 1, 0.2 ml, etc) and 7-ml centrifuge tubes were cleaned in an ultra-clean laboratory according to the method described in Zhu *et al.* (2018).

Twenty-six geological reference materials were used to determine Ni isotopes in this study. Among them, BHVO-2 (basalt), BCR-2 (basalt), JP-1 (Peridotite), PCC-1 (Peridotite), SGR-1b (shale) and CLB-1 (coal) were purchased from the United States Geological Survey (USGS). The remainder, including igneous rocks (GSR-2, GSR-3), sedimentary rocks (GSR-4, GSR-5, GSR-6), stream sediments (GSD-1, GSD-3, GSD-9, GSD-10, GSD-11) and soils (GSS-1, GSS-2, GSS-3, GSS-4, GSS-5, GSS-6, GSS-7, ESS-1), as well as plants (GSB-4, GSB-12), were acquired from the Institute of Geophysical and Geochemical Research (IGGE) of the Chinese Academy of Geological Sciences.

Sample digestion

To completely digest the various samples, digestion methods fully described in Zhu *et al.* (2018) were used. Briefly, approximately 50 mg of peridotite, basalt or andesite powders were digested in 15-ml PFA beakers using concentrated HNO_3 (15.8 mol l^{-1}) and HF (23 mol l^{-1}, 1:2 by volume) on a hot plate at 140 °C. During sample decomposition, ultrasound treatment and heating were repeated until clear solutions were achieved. The solutions were then evaporated to near dryness. Following this, 3 ml of *aqua regia* (HNO_3:HCl = 1 ml:3 ml) was added and solutions were placed on a hot plate at 130 °C until sample residues were completely dissolved. Shale, soil and stream sediment samples were digested with customised high-

Table 1.
Nickel mass fraction and isotope composition of geological reference materials

Reference material	Sample type	Reference	Source [a]	Ni (μg g^{-1})	$\delta^{60/58}$Ni [b]	2*s* [c]	*N* [d]
PCC-1	Peridotite	This study	USGS	2362	0.12 [e]	0.06 [c]	2
					0.13 [f]	0.06 [c]	2
					0.13 [g]	0.05	5
					0.13 [h]	0.05	5
					0.12 [i]	0.03	4
		Gueguen *et al.* (2013)		2245	0.119	0.045	5
		Chemonozhkin *et al.* (2015)		–	0.166	0.048	8
		Gall *et al.* (2017)		2325	0.141	0.056	17
JP-1		This study	USGS	2480	0.13 [e]	0.03	3
					0.14 [f]	0.04	4
					0.13 [g]	0.03	9
					0.13 [h]	0.03	9
					0.13 [i]	0.03	7
		Chemonozhkin *et al.* (2015)		–	0.134	0.029	1
		Steele *et al.* (2011)		–	0.100	0.08	54
		Wu *et al.* (2019)		2480	0.18	0.05	6
BHVO-2	Basalt	This study	USGS	115	0.02 [f]	0.04	3
					0.03 [g]	0.02	3
					0.03 [h]	0.02	3
		Estrade *et al.* (2015)			-0.01	0.05	11
		Gueguen *et al.* (2013)			0.006	0.04	11
		Ratié *et al.* (2015)			0.05	0.11	–
		Chemonozhkin *et al.* (2015)			0.083	0.019	5
		Cameron *et al.* (2009)		–	0.13	0.03	–
		Wu *et al.* (2019)		115	0.03	0.06	6
BCR-2		This study	USGS	9.5	0.26 [e]	0.06 [c]	1
					0.21 [f]	0.06 [c]	2
					0.22 [g]	0.04	4
					0.22 [h]	0.04	4
					0.23 [i]	0.04	3
		Cameron *et al.* (2009)		–	0.20	0.07	–
		Wu *et al.* (2019)		9.5	0.21	0.06	5
GSR-3		This study	IGGE	140	-0.03 [f]	0.06 [c]	2
					-0.04 [g]	0.06	3
					-0.04 [h]	0.06	3
		Wu *et al.* (2019)			-0.03	0.06	3
GSR-2	Andesite	This study	IGGE	17	0.19 [e]	0.06 [c]	1
					0.17 [f]	0.06 [c]	2
					0.15 [g]	0.06 [c]	1
					0.15 [h]	0.06 [c]	1
					0.17 [i]	0.04	3
		Wu *et al.* (2019)			0.18	0.02	3
GSR-4	Quartz Sandstone	This study	IGGE	16.6	0.09 [f]	0.06 [c]	2
					0.11 [g]	0.04	3
					0.10 [h]	0.04	3
GSR-5	Shale	This study	IGGE	37	0.10 [f]	0.06 [c]	2
					0.08 [g]	0.04	3
					0.08 [h]	0.03	3
SGR-1b		This study	USGS	29	0.56 [f]	0.04	4

Table 1 (continued).
Nickel mass fraction and isotope composition of geological reference materials

Reference material	Sample type	Reference	Source [a]	Ni (μg g^{-1})	$\delta^{60/58}$Ni [b]	2*s* [c]	*N* [d]
					0.53 [g]	0.06 [c]	2
					0.52 [h]	0.06 [c]	2
		Wu *et al.* (2019)			0.54	0.06	5
CLB-1	coal	This study	USGS	19	0.47 [f]	0.06	8
					0.48 [g]	0.06	2
					0.48 [h]	0.06	2
		Gueguen *et al.* (2013)			0.473	0.048	4
GSR-6	Argillaceous limestone	This study	IGGE	18	0.16 [e]	0.06 [c]	1
					0.15 [f]	0.06 [c]	2
					0.14 [g]	0.06 [c]	2
					0.14 [h]	0.06 [c]	2
					0.16 [i]	0.02	3
GSD-1	Stream sediment	This study	IGGE	76	0.22 [f]	0.06 [c]	2
					0.19 [g]	0.06 [c]	1
					0.18 [h]	0.06 [c]	1
GSD-3		This study	IGGE	26	0.10 [e]	0.06 [c]	1
					0.12 [f]	0.06 [c]	2
					0.12 [g]	0.02	3
					0.11 [h]	0.02	3
					0.12 [i]	0.02	3
GSD-9		This study	IGGE	32	0.17 [e]	0.06 [c]	1
					0.18 [f]	0.04	3
					0.15 [g]	0.06 [c]	2
					0.15 [h]	0.06	2
					0.18 [i]	0.04	4
GSD-10		This study	IGGE	30	0.46 [f]	0.06	3
					0.46 [g]	0.04	3
					0.46 [h]	0.03	3
GSD-11		This study	IGGE	14.3	0.16 [e]	0.06 [c]	1
					0.18 [f]	0.06 [c]	2
					0.17 [g]	0.03	3
					0.17 [h]	0.03	3
					0.18 [i]	0.03	3
GSS-1	soil	This study	IGGE	20.4	-0.27 [f]	0.06 [c]	1
					-0.29 [g]	0.06 [c]	2
					-0.29 [h]	0.06 [c]	2
GSS-2		This study	IGGE	19.4	0.03 [f]	0.06 [c]	2
					0.05 [g]	0.02	3
					0.05 [h]	0.02	3
GSS-3		This study	IGGE	12	0.12 [f]	0.06 [c]	2
					0.09 [g]	0.05	3
					0.11 [h]	0.02	3
GSS-4		This study	IGGE	64	0.17 [f]	0.06 [c]	2
					0.16 [g]	0.03	3
					0.16 [h]	0.03	3
GSS-5		This study	IGGE	40	0.06 [e]	0.06 [c]	1
					0.04 [f]	0.06 [c]	2
					0.06 [g]	0.02	3
					0.05 [h]	0.03	3
					0.05 [i]	0.02	3
GSS-6		This study	IGGE	53	0.17 [f]	0.06 [c]	2
					0.19 [g]	0.06 [c]	1
					0.19 [h]	0.06 [c]	1
GSS-7		This study	IGGE	276	-0.11 [f]	0.01	3
					-0.09 [g]	0.03	3
					-0.10 [h]	0.04	3

Table 1 (continued).
Nickel mass fraction and isotope composition of geological reference materials

Reference material	Sample type	Reference	Source [a]	Ni (μg g^{-1})	$\delta^{60/58}$Ni [b]	2*s* [c]	*N* [d]
ESS-1		This study	IGGE	30	0.05 [f]	0.06 [c]	1
					0.01 [g]	0.06 [c]	1
					0.02 [h]	0.06 [c]	1
GSB-4	Soybean	This study	IGGE	4.0	0.13 [f]	0.01	4
GSB-12	Bean	This study	IGGE	4.4	0.52 [f]	0.06	4

– no data available.
[a] USGS: United States Geological Survey; IGGE: Institute of Geophysical and Geochemical Research of the Chinese Academy of Geological Sciences.
[b] All the reference data were re-normalised relative to NIST SRM 986
[c] Precision was represented by 0.06 (2*s*) as a long-term 'external' because samples were measured independently twice or once.
[d] Time of repeat analyses for reference materials.
[e] On-peak zero (OPZ), samples were determined on Nu Plasma III.
[f] Electrostatic analyser (ESA) deflection, samples were determined on Nu Plasma III.
[g] OPZ, samples were determined on Neptune Plus.
[h] Without OPZ, samples were determined on Neptune Plus.
[i] Mean of both OPZ and ESA for Nu Plasma III.

pressure bombs. Test portion powders (~ 100 mg) were weighed into 30-ml PTFE-lined vials for digestion, and a 3.2 ml mixture of 0.5–0.8 ml HF and 2.4–2.7 ml HNO_3 was added. The sealed bombs were placed in an oven and heated for 48 h at 185 ± 5 °C. To achieve complete digestion, the processes were repeated twice in bombs. For plant materials, the digestion procedure was similar to that for shale; 0.2 ml HF was used in the digestion. For carbonate samples, ~ 100 mg powder test portions were also weighed into high-pressure bombs, and 1 ml HPW and 0.5 ml of 6 mol l^{-1} HCl were added. After degassing for 1–2 h, the samples were evaporated. The samples were then mixed with 3.2 ml of 15.6 mol l^{-1} HNO_3 and digested in bombs at 185 ± 5 °C for 12 h. All the above completely decomposed samples were dissolved in 1 ml 10% *v/v* HNO_3 (HNO_3:HPW = 10 ml:90 ml) in beakers and transferred into the pre-cleaned 7-ml tubes for later chemical purification.

Chromatographic separation

The purification of all samples was carried out under a class 100 hood in an ultra-clean laboratory (1000 class) in the Laboratory of Surficial Environmental Geochemistry of China University of Geosciences (Beijing, China). In a similar way to previous studies (Wang *et al.* 2019, Wu *et al.* 2019), the double-spike method was used to calibrate potential isotope fractionation during purification and measurement. Before purification, samples containing 600–800 ng Ni were spiked with a suitable amount of a double spike (^{61}Ni-^{62}Ni) to obtain a ratio of $^{62}Ni_{spike}/^{58}Ni_{sample} \approx 1.3$ (Wu *et al.* 2019). The mixed sample solutions were sealed and heated overnight on a hot plate at 100 °C to equilibrate spike and sample.

As described in Wu *et al.* (2019), the purification included four steps used to separate Ni from matrix elements. Step I consisted of two consecutive columns. Sample Ni were sequentially passed through 2 ml of AG50W-X8 (200–400 mesh) and 2 ml of AG1-X8 (100–200 mesh) resins pre-conditioned with HCl, to remove Ca and Fe. In Step II, samples dissolved in 0.15 mol l^{-1} HNO_3 and 4 mol l^{-1} HF were loaded onto preconditioned 1 ml quantities of AG50W-X8 (200–400 mesh) resin. This step was able to remove matrix elements such as Mg, Ti and Al. In Step III, under 0.5 mol l^{-1} HCl and 95% *v/v* acetone (10 mol l^{-1} HCl:Acetone = 5 ml:95 ml) conditions, Ni was adsorbed in 1 ml of AG50W-X8 resin (200–400 mesh) and Mn was directly eluted from the resin. Step IV utilised the strong complexation between Ni^{2+} and Dimethylglyoxime (DMG). Residual matrix elements were cleaned with 1 ml of AG50W-X8 resin (200–400 mesh). Finally, in order to achieve high purity Ni and further eliminate possible organic matter, steps I and IV were repeated. Purified Ni samples were evaporated to dryness and re-dissolved in 2% *v/v* HNO_3 (HNO_3:HPW = 2 ml:98 ml) for isotope ratio measurements.

Mass spectrometry

Following previously published procedures for measuring Ni isotopes (Wu *et al.* 2019), Ni isotope ratios were determined using a Nu Plasma III MC-ICP-MS (Nu III) at the Surface Environmental Geochemistry Laboratory of China University of Geosciences (Beijing). This instrument was equipped with sixteen Faraday cups. Each of the cups was connected to a 10^{11} Ω resistor. The measurement was conducted through nine Faraday cups (Table 2): ^{57}Fe (L5), ^{58}Ni (L4), ^{59}Co (L2), ^{60}Ni (Ax), ^{61}Ni (H2), ^{62}Ni (H4), ^{63}Cu

(H6), ^{64}Ni (H7) and ^{65}Cu (H8). In addition, in order to check whether the $\delta^{60/58}$Ni values showed any difference between OPZ and ESA models, the measurement of Ni isotope ratios in geological RMs were also performed on a Neptune Plus MC-ICP-MS (NP) at the Isotope Geochemistry Laboratory, China University of Geosciences (Beijing). The Neptune Plus MC-ICP-MS was equipped with nine Faraday cups connected with 10^{11} Ω resistor amplifiers. Nickel isotopes were measured using seven Faraday cups (Table 2). The typical operating conditions of the two instruments including cup configuration, cones, gas flow rate and others are listed in Table 2. In this study, unlike several previous studies reported in Gueguen *et al.* (2013), Ventura *et al.* (2015) and Gall *et al.* (2017), the isotope ratios of all samples were measured on both instruments under static mode and low-resolution mode. To correct the isobaric effect of Fe, ^{57}Fe was monitored using L5 for Nu III and L3 for NP so that ^{58}Fe could be subtracted using an assumed ^{57}Fe/^{58}Fe ratio.

Purified samples and standard solutions were commonly run at a concentration of 100 μg l^{-1} Ni in 2% *v/v* HNO_3 and introduced into the plasma by an Aridus III/II desolvating sample introduction system equipped with a 100 μl min^{-1} micro-concentric PFA nebuliser (ESI, USA) for Nu III and ~ 110 μl min^{-1} for NP. The signal intensity of ^{60}Ni (central cup) was ≥ 2.5 V for Nu III and ≥ 10 V for NP. Each isotopic measurement of a sample and standard solution included three blocks with thirty cycles (Table 2). Electronic baselines were conducted by ESA deflection at 20 V for 30 s before running each block on Nu III, and several geological RMs were also determined at on-peak zero to compare $\delta^{60/58}$Ni values with the obtained data from the ESA model, while $\delta^{60/58}$Ni values in geological RMs (except GSB-4 and 12) measured on NP were achieved with and without blank subtraction (Figure S1). Prior to starting each measurement session, the sample introduction system was washed with 2% *v/v* HNO_3 until the ^{61}Ni signal dropped to < 2 mV on Nu III and < 5 mV on NP. The blank of 2% *v/v* HNO_3 was then measured at the peak and subtracted from subsequent sample signals. Blank contributions generally accounted for < 0.25‰ on Nu III and < 0.2‰ on NP for the signal intensity of ^{61}Ni, which was similar to values reported in Cameron *et al.* (2009). Therefore, the contribution of blank signal to the Ni isotopic ratios was negligible, and there was not significant a difference in $\delta^{60/58}$Ni values obtained with the OPZ and ESA models (Table 2). Meanwhile, a spiked NIST SRM 986 standard solution was measured immediately before and after each batch of three to five samples to monitor the stability of the instrument. All results were reported relative to NIST SRM 986 as δ (‰) (Coplen 2011):

Table 2.
Instrument parameters for Ni isotope measurements

Parameter	Settings for Nu III	Settings for NP
Cup configuration	L5(^{57}Fe), L4(^{58}Ni), L2 (^{59}Co), Ax(^{60}Ni) H2 (^{61}Ni), H4(^{62}Ni), H6 (^{63}Cu), H7(^{64}Ni), H8 (^{65}Cu), H9(^{66}Zn)	NP main run: L3(^{57}Fe), L2(^{58}Ni), C(^{60}Ni), H1 (^{61}Ni), H2(^{62}Ni), H4 (^{64}Ni) NP interf. run: C(^{62}Ni), H4(^{66}Zn)
RF power	1300 W	1250 W
Sampler cone	Ni, wet type	Pt cone (H)
Skimmer cone	Ni, wet type	Pt cone (X)
Cooling Ar flow rate	13.5 l min^{-1}	15 l min^{-1}
Auxiliary Ar flow rate	0.85 min^{-1}	0.70 l min^{-1}
Nebuliser Ar flow rate	25.0 psi	25.0 psi
Resolution mode	Low	Low
Spray chamber temperature	110 °C	110 °C
Desolator temperature	140 °C	160 °C
Ar sweep gas	5.46 l min^{-1}	2.85 l min^{-1}
Nitrogen gas	No	18 ml min^{-1}
Sample uptake rate	100 μl min^{-1}	110 μl min^{-1}
Blocks per analysis	3	3
Cycles per block	10	10
Cycle integration time	10 s	4.194 s
Sensitivity of ^{60}Ni	25 μg g^{-1}	100 μg g^{-1}

$$\delta^{60/58}Ni_{NIST\ SRM\ 986} = (((^{60}Ni/^{58}Ni)_{sample} / (^{60}Ni/^{58}Ni)_{NIST\ SRM\ 986}) - 1 \quad (1)$$

We observed that the $\delta^{60/58}$Ni value of the spiked NIST SRM 986 occasionally had a small constant shift (Wu *et al.* 2019). Thus, sample $\delta^{60/58}$Ni values were normalised to the mean of bracketing NIST SRM 986 RMs by $\delta^{60/58}Ni_{corrected\text{-}sample} = \delta^{60/58}Ni_{\ sample} - \delta^{60/58}Ni_{\ NIST\ SRM\ 986}$.

Results and discussion

Blank contributions

The total procedural blank of Ni, including sample digestion to separation of all columns, ranged from 1.13 to 1.49 ng with a mean of 1.3 ± 0.3 ng (2*s*, *n* = 3), which was within the range (0.9–4 ng) of Ni blank reported in previous studies (Gueguen *et al.* 2013, Deng *et al.* 2014, Ciscato *et al.* 2018, Spivak-Birndorf *et al.* 2018, Wu *et al.* 2019). Our Ni blanks only accounted for approximately 0.2% of the test portion sizes (600–800 ng Ni). In addition, Wu *et al.* (2019) demonstrate that the effects (~ 0.6%) of < 1.2 ng blank on the whole separation procedure of samples containing 200 ng Ni was negligible. Our procedural blank therefore would not affect the Ni isotope ratio.

Evaluation of isobaric interferences and matrix effects

The effects of matrix elements and isobaric interferences on the measurement of Ni isotope ratios have been evaluated in detail in previous studies (Cameron *et al.* 2009, Gall *et al.* 2012, Gueguen *et al.* 2013, Chernonozhkin *et al.* 2015, Wu *et al.* 2019). Those results show that the matrix effects and/or isobaric interferences on the $\delta^{60/58}$Ni values can be neglected when the ratios of [Ca]/[Ni], [Na]/[Ni], [Cr]/[Ni], [Ti]/[Ni] and [Fe]/[Ni] were generally less than 0.5 (Gall *et al.* 2012, Gueguen *et al.* 2013, Chernonozhkin *et al.* 2015, Wu *et al.* 2019). However, since it is suspected that a very small amount of organic matter may remain in the purified solution, the spiked Ni standard solutions (NIST SRM 986) through purification were doped with different proportions of Ti, Cr, V and Fe to evaluate the effects of polyatomic ion interferences (e.g., $^{48}Ti^{12}C^{+}$ $^{50}Cr^{12}C^{+}$ and $^{50}V^{12}C^{+}$) on Ni isotope measurements. Figure 1 shows that $\delta^{60/58}$Ni values did not deviate from the 'true' value when the ratios of [Cr]/[Ni], [Ti]/[Ni], [V]/[Ni] and [Fe]/[Ni] were ≤ 0.5. This observation is consistent with that presented in Gall *et al.* (2012) and Wu *et al.* (2019), indicating that the influence of Cr, Ti, V and Fe on $\delta^{60/58}$Ni value was negligible in our study.

Measurement precision and accuracy

Isotope standard solutions (NIST SRM 986) and geological RMs were repeatedly used to evaluate the long-term 'external' precision and accuracy of Ni isotope ratios. The intermediate precision was obtained by measuring spiked NIST SRM 986 over the past six months (Figure 2). The two standard deviation (2*s*) value of results was 0.05‰ (*n* = 69), which was close to previous studies (Gall *et al.* 2012, Gueguen *et al.* 2013, Ratié *et al.* 2016, Wu *et al.* 2019). Geological RMs including BHVO-2, GSD-10, GSB-4, GSB-12, SGR-1b and CLB-1 were repeatedly measured, and their intermediate ('external') precisions were 0.04‰ (2*s*, *n* = 3), 0.06‰ (2*s*, *n* = 3), 0.01‰ (2*s*, *n* = 4), 0.06‰ (2*s*, *n* = 4), 0.04‰ (2*s*, *n* = 4) and 0.06‰ (2*s*, *n* = 8), respectively, consistent with previous works (Gueguen *et al.* 2013, Chernonozhkin *et al.* 2015, Ratié *et al.* 2015, Estrade *et al.* 2015, Wu *et al.* 2019). The results of these analyses showed that the method was high precision and the 'long-term' precision of $\delta^{60/58}$Ni for actual samples was ± 0.06‰.

A standard solution (NIST SRM 986) and several geological RMs with published data were used to evaluate the accuracy of our methods further. The long-term measured result for NIST SRM 986 was 0.00 ± 0.05‰ (2*s*, *n* = 69).

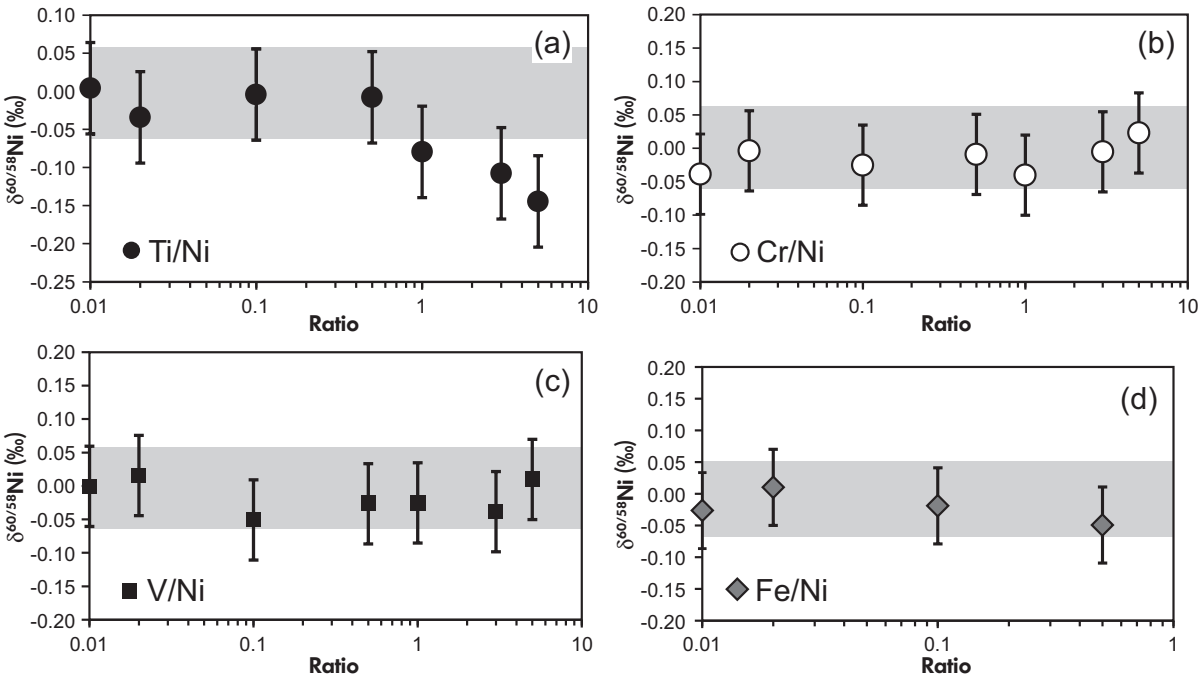

Figure 1. Effects of different elements with varied ratios of [X]/[Ni] (X = V, Cr, Ti and Fe) on $\delta^{60/58}$Ni values (NIST SRM 986). Vertical range bars (2*s*) = 0.06‰.

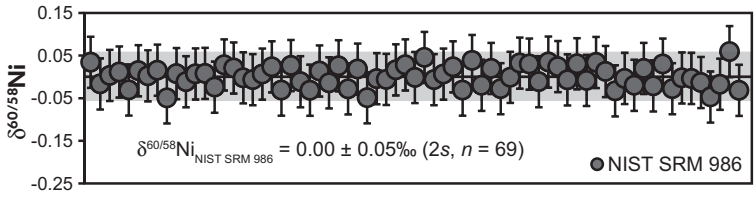

Figure 2. The intermediate precision of $\delta^{60/58}$Ni for NIST SRM 986.

Geological RMs BHVO-2, BCR-2, JP-1, PCC-1 and CLB-1 were digested and analysed multiple times. Their analytical accuracy was 0.02 ± 0.04‰ (2*s*, *n* = 3), 0.23 ± 0.04‰ (2*s*, *n* = 3), 0.13 ± 0.03‰ (2*s*, *n* = 7), 0.12 ± 0.03‰ (2*s*, *n* = 4) and 0.47 ± 0.06‰ (2*s*, *n* = 8), respectively. Detailed results of real samples are shown in Table 1 and Figure 3, which clearly showed that our results were in good agreement with previously reported values (Cameron *et al.* 2009, Steele *et al.* 2011, Gueguen *et al.* 2013, Chernonozhkin *et al.* 2015, Estrade *et al.* 2015, Ratié *et al.* 2015, Gall *et al.* 2017, Wu *et al.* 2019).

Ni isotope composition in geological reference materials

The Ni isotope compositions of twenty-six geological RMs are presented in Table 1 and Figure 4, together with literature data for comparison. In the following paragraphs, the Ni isotope compositions of reference materials of five groups (igneous rock, sedimentary rock, sediments, soil and plants) will be discussed in detail.

Igneous rock reference materials: The $\delta^{60/58}$Ni value of peridotite JP-1 was 0.13 ± 0.03‰ (2*s*, *n* = 7; Table 1 and Figure 4), in excellent agreement with 0.134 ± 0.029‰ (2*s*, *n* = 1) by Chernonozhkin *et al.* (2015) and 0.100 ± 0.08‰ (2*s*, *n* = 54) by Steele *et al.* (2011). Similarly, the $\delta^{60/58}$Ni value of another peridotite (PCC-1) was measured at 0.12 ± 0.03‰ (2*s*, *n* = 4), which is identical to 0.119 ± 0.045‰ (2*s*, *n* = 5) reported by Gueguen *et al.* (2013), 0.166 ± 0.048‰ (2*s*, *n* = 8) reported by Chernonozhkin *et al.* (2015) and 0.141 ± 0.056‰ (2*s*, *n* = 17) determined by Gall *et al.* (2017). For the basalt RMs, our result for the $\delta^{60/58}$Ni value of BCR-2 was 0.23 ± 0.04‰ (2*s*, *n* = 3), which is similar to 0.20 ± 0.07‰ (2*s*) reported by Cameron *et al.* (2009) and 0.21 ± 0.06‰ (2*s*, *n* = 5) determined by Wu *et al.* (2019). The $\delta^{60/58}$Ni value of basalt BHVO-2 was 0.02 ± 0.04‰ (2*s*, *n* = 3), which is in the range (-0.01‰ to 0.13‰) reported in previous studies (Cameron *et al.* 2009, Gueguen *et al.* 2013, Chernonozhkin *et al.* 2015, Estrade *et al.* 2015, Ratié *et al.* 2016, Wu *et al.* 2019). The $\delta^{60/58}$Ni value of basalt GSR-3 was -0.03 ± 0.06 (2*s*, *n* = 2; Table 1

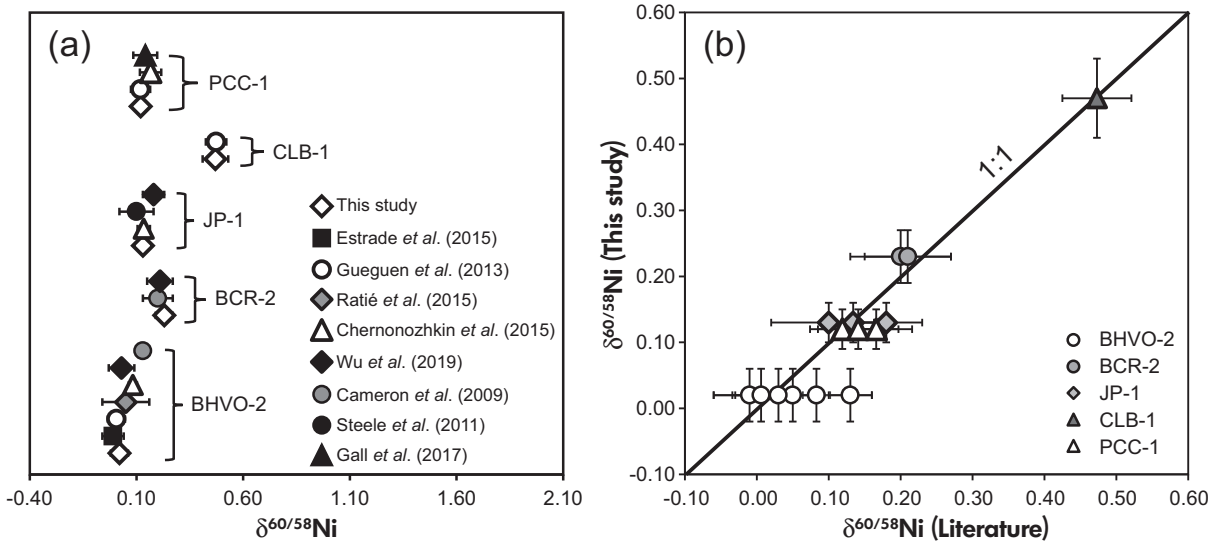

Figure 3. Interlaboratory comparison of $\delta^{60/58}$Ni values for chosen geological reference materials. (a) Comparison of published data with references. (b) Correlation between this study and previous studies.

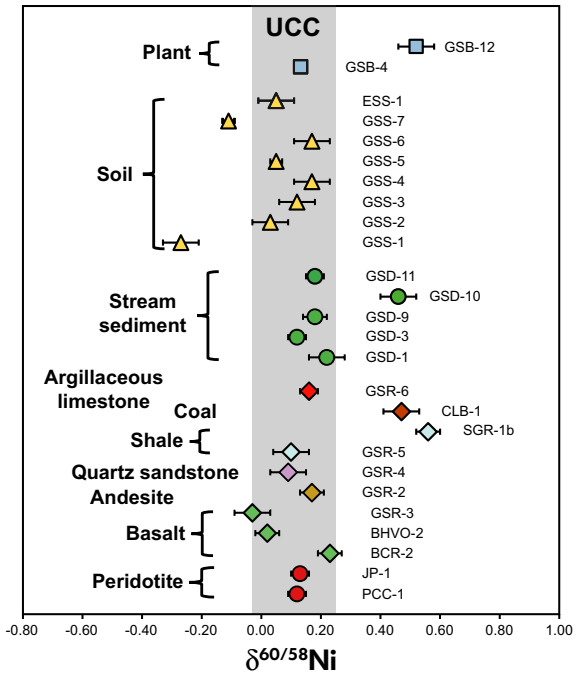

Figure 4. $\delta^{60/58}$Ni values for selected geological reference materials analysed in this study. The grey vertical bar represents the Ni isotope composition (0.11 ± 0.14‰) of the Upper Continental Crust (preliminary estimation of Wu *et al.* 2019). [Colour figure can be viewed at wileyonlinelibrary.com]

and Figure 4) in this study, consistent with -0.03 ± 0.06‰ (2*s*, *n* = 3) presented by Wu *et al.* (2019). In addition, compared with the reported geological RMs of basalt such as BCR-2 (0.20 ± 0.07‰, 0.21 ± 0.07‰), BIR-1 (0.12 ± 0.14‰, 0.19 ± 0.07‰) and JB-2 (0.26 ± 0.03‰) (Cameron *et al.* 2009, Gueguen *et al.* 2013, Chernonozhkin *et al.* 2015, Wu *et al.* 2019), GSR-3 and BHVO-2 had lighter Ni isotope compositions.

For the andesite rock RM GSR-2, the $\delta^{60/58}$Ni value was 0.17 ± 0.04‰ (2*s*; Table 1 and Figure 4), similar to 0.18 ± 0.02‰ reported for GSR-2 by Wu *et al.* (2019). It was heavier than AGV-2 (0.02 ± 0.01‰, Wu *et al.* 2019) and lower than JA-1 (0.33 ± 0.1‰, Cameron *et al.* 2009).

Sedimentary rock reference materials: The $\delta^{60/58}$Ni values of shale GSR-5 and SGR-1b were 0.10 ± 0.06‰ (2*s*, *n* = 2) and 0.56 ± 0.04‰ (2*s*, *n* = 4), respectively (Table 1 and Figure 4). The former was consistent with 0.08 ± 0.08‰ (2*s*, *n* = 8) of SCo-1 determined by Wang and Wasylenki (2017) and was in the range 0.04–0.16‰ reported by Gall *et al.* (2012). The latter was in agreement with SGR-1b (0.54 ± 0.06‰) presented by Wu *et al.* (2019) and SGR-1 (0.66 ± 0.06‰) obtained by Ventura *et al.* (2015) and was similar to SDo-1 (0.54–0.61‰) (Gueguen *et al.* 2013, Estrade *et al.* 2015, Wang and Wasylenki 2017, Wu *et al.* 2019). Another sample containing high contents of organic matter – CLB-1 coal – gave $\delta^{60/58}$Ni values of 0.47 ± 0.06‰ (2*s*, *n* = 8; Table 1 and Figure 4), which agrees with 0.473 ± 0.048‰ presented by Gueguen *et al.* (2013). So far, a large range of Ni isotopic composition (-0.84‰ to 2.5‰) was estimated from the black shale and organic-rich sediments, with a median of 0.56‰ (*n* = 78) and a mean of 0.55 ± 1.31‰ (2*s*, *n* = 78) (Porter *et al.* 2014, Ciscato *et al.* 2018, Pašava *et al.* 2018). The $\delta^{60/58}$Ni values of GSR-5 and SGR-1b in this study were in the range reported in the literature.

Currently, to the best of our knowledge, carbonate rocks have been reported rarely, only one sample having been published for JDo-1 (0.82 ± 0.09‰, 2*s*, Wu *et al.* 2019). In this study, the $\delta^{60/58}$Ni value of GSR-6 (argillaceous limestone) was reported for the first time to be 0.16 ± 0.02‰ (2*s*, *n* = 3; Table 1 and Figure 4), being slightly lower than that of JDo-1. Quartz sandstone (GSR-4) as a typical sedimentary rock was first determined, with the $\delta^{60/58}$Ni value of 0.09 ± 0.06‰ (2*s*, *n* = 2; Table 1 and Figure 4), which was close to GSR-5 reported in this study.

Sediment reference materials: In this study, the $\delta^{60/58}$Ni values of five stream sediments, GSD-1, GSD-3, GSD-9, GSD-10 and GSD-11, were measured (Table 1 and Figure 4): 0.22 ± 0.06‰ (2*s*, *n* = 2), 0.12 ± 0.02‰ (2*s*, *n* = 3), 0.18 ± 0.04‰ (2*s*, *n* = 4), 0.46 ± 0.06‰ (2*s*, *n* = 3) and 0.18 ± 0.03‰ (2*s*, *n* = 3), respectively. Notably, the $\delta^{60/58}$Ni value of GSD-10 collected from a carbonate source area was much higher than the values for all reported stream sediments. The isotope composition of this sample may be affected by the characteristics of the parent rock, because carbonate rocks have abnormal Ni isotope compositions according to the results of theoretical calculations and sample measurements (Fujii *et al.* 2011, Wu *et al.* 2019). In previous studies, the five stream sediments had $\delta^{60/58}$Ni values ranging from 0.07‰ to 0.24‰, with a median of 0.15‰ and a mean of 0.16‰ (Cameron *et al.* 2009, Wu *et al.* 2019). Compared with these previously reported values, on average the results of $\delta^{60/58}$Ni (0.23 ± 0.24‰, 2*s*, *n* = 5) represents a slightly heavy Ni isotope composition. According to the data presented by Cameron *et al.* (2009) and Wu *et al.* (2019), the $\delta^{60/58}$Ni values of stream sediment samples have a large range (from 0.07‰ to 0.46‰), which suggest that the relevant material

source may have a large influence on Ni isotope composition.

Soil reference materials: The $\delta^{60/58}$Ni values of the soils (GSS-1–7 and ESS-1) varied from -0.27‰ to 0.17‰ (Table 1 and Figure 4), with a mean value of 0.03 ± 0.28‰ (2*s*, *n* = 8). Among them, GSS-1 (-0.27 ± 0.06‰) and GSS-7 (-0.11 ± 0.01‰) taken from a weathered basalt unit were lower than other soils reported in this study. In previous research, the published $\delta^{60/58}$Ni values of other soil reference materials (GSS-9–12, 14–16) reported by Wu *et al.* (2019) were from -0.02‰ to 0.17‰, which was in the range of our reported values. Similarly, the $\delta^{60/58}$Ni values of NIST SRM 2711 and NIST SRM 2711a were 0.14 ± 0.02‰ (2*s*) and 0.16 ± 0.06‰ (2*s*, *n* = 3), respectively, in previous research (Gueguen *et al.* 2013 and Wu *et al.* 2019) and were heavier than our mean results. Currently, natural soil samples showed highly variable $\delta^{60/58}$Ni signatures varying from -0.61‰ to 1.71‰, with a median of -0.06‰ (*n* = 57) and a mean of 0.08 ± 0.90‰ (2*s*, *n* = 57) (Gall *et al.* 2013, Ratié *et al.* 2015, 2016, Estrade *et al.* 2015, Šillerová *et al.* 2017). Our reported data fall within the range of Ni isotope values reported in the literature (Gall *et al.* 2013, Ratié *et al.* 2015, 2016, Estrade *et al.* 2015, Šillerová *et al.* 2017).

Plant reference materials: For the RMs of plants, the $\delta^{60/58}$Ni values of GSB-4 (Soybean) and GSB-12 (Bean) were 0.13 ± 0.01‰ (2*s*, *n* = 4) and 0.51 ± 0.08‰ (2*s*, *n* = 4), respectively (Table 1 and Figure 4), which were in the range of previous studies (-0.05‰ to 0.65‰; Estrade *et al.* 2015). However, the $\delta^{60/58}$Ni value of hyper-accumulated and non-accumulated plants that were cultured in nutrient solution (-0.10 ± 0.13‰) was estimated to be -0.52 ± 0.72‰ (2*s*, *n* = 18) (Deng *et al.* 2014). This value was much lower than GSB-4 and GSB-12. Since GSB-12 (0.51 ± 0.08‰) was obviously heavy, these could serve as better references for Ni isotope fractionation.

Conclusions

This study presents a set of Ni isotope compositions of a range of geological and environmental reference materials. The Ni isotope ratios of all geological RMs were measured using a ^{61}Ni-^{62}Ni double spike by MC-ICP-MS (Nu Plasma III). To evaluate the measurement bias and intermediate precision of data, a spiked NIST SRM 986 RM, BHVO-2, BCR-2, JP-1, PCC-1 and CLB-1 were analysed. The intermediate precision of $\delta^{60/58}$Ni values determined in this work was 0.05‰ (2*s*, *n* = 69) for NIST SRM 986 and 0.06‰ for geological RMs. The $\delta^{60/58}$Ni values of BHVO-2, BCR-2, JP-1, PCC-1 and CLB-1 were 0.02 ± 0.04‰ (2*s*, *n* = 3), 0.23 ± 0.04‰ (2*s*, *n* = 3), 0.13 ± 0.03‰ (2*s*, *n* = 7), 0.12 ± 0.03‰ (2*s*, *n* = 4) and 0.47 ± 0.06‰ (2*s*, *n* = 8), respectively, which were consistent with those in previous studies. Eighteen Ni isotope ratios were reported for the first time, and the $\delta^{60/58}$Ni values varied from -0.27‰ to 0.52‰, with a mean of 0.13 ± 0.34‰ (2*s*, *n* = 18). Apart from SGR-1b (0.56 ± 0.04‰, 2*s*), GSS-1 (-0.27 ± 0.06‰, 2*s*), GSS-7 (-0.11 ± 0.01‰, 2*s*), GSD-10 (0.46 ± 0.06‰, 2*s*), GSB-12 (0.52 ± 0.06‰, 2*s*) and CLB-1 (0.47 ± 0.06‰, 2*s*), the other geological RMs, including igneous and sedimentary rocks, stream sediments, soils and plant reference materials, were almost entirely within the range of upper continental crust composition (0.11 ± 0.14‰; Figure 3) reported by Wu *et al.* (2019). Additionally, due to the clearly characteristic Ni isotope composition of SGR-1b, GSS-1, GSS-7, GSD-10 and GSB-12 revealed in this study, these could be used as potential reference materials for future quality control and interlaboratory comparison of Ni isotope compositions in natural samples.

Acknowledgements

This study was supported by the National Natural Science Foundation of China (Nos. U1612441, 41673017) and MOST Special Fund from the State Key Laboratory of Geological Processes and Mineral Resources, China University of Geosciences (MSFGPMR201812). We would like to thank Dr. Johnson at the University of Illinois for providing help in calibrating the double spike and Dr. Lei Meng at Western Michigan University for providing help in English polishing.

Conflicts of interest

There are no conflicts of interest to declare.

Data availability statement

The data that support the findings of this study are available from the corresponding author upon reasonable request.

References

Barnett S. (2010)
Nickel – A key material for innovation in a sustainable future. In: 2nd Euro Nickel Conference. Informa Pty Ltd (London, UK), 32pp.

Cameron V. and Vance D. (2014)
Heavy nickel isotope compositions in rivers and the oceans. Geochimica et Cosmochimica Acta, 128, 195–211.

references

Cameron V., Vance D., Archer C. and House C.H. (2009)
A biomarker based on the stable isotopes of nickel. Proceedings of the National Academy of Sciences of the United States of America, 106, 10944–10948.

Chernonozhkin S.M., Goderis S., Lobo L., Claeys P. and Vanhaecke F. (2015)
Development of an isolation procedure and MC-ICP-MS measurement protocol for the study of stable isotope ratio variations of nickel. Journal of Analytical Atomic Spectrometry, 30, 1518–1530.

Ciscato E.R., Bontognali T.R. and Vance D. (2018)
Nickel and its isotopes in organic-rich sediments: Implications for oceanic budgets and a potential record of ancient seawater. Earth and Planetary Science Letters, 494, 239–250.

Coplen T.B. (2011)
Guidelines and recommended terms for expression of stable-isotope-ratio and gas-ratio measurement results. Rapid Communications in Mass Spectrometry, 25, 2538–2560.

Deng T.H.B., Cloquet C., Tang Y.T., Sterckeman T., Echevarria G., Estrade N. and Qiu R.L. (2014)
Nickel and zinc isotope fractionation in hyperaccumulating and nonaccumulating plants. Environmental Science and Technology, 48, 11926–11933.

Denkhaus E. and Salnikow K. (2002)
Nickel essentiality, toxicity, and carcinogenicity. Critical Reviews in Oncology/Hematology, 42, 35–56.

Dixon N.E., Gazzola C., Blakeley R.L. and Zerner B. (1975)
Jack bean urease (EC 3.5. 1.5). Metalloenzyme. Simple biological role for nickel. Journal of the American Chemical Society, 97, 4131–4133.

Elliott T. and Steele R.C. (2017)
The isotope geochemistry of Ni. Reviews in Mineralogy and Geochemistry, 82, 511–542.

Estrade N., Cloquet C., Echevarria G., Sterckeman T., Deng T., Tang Y. and Morel J.L. (2015)
Weathering and vegetation controls on nickel isotope fractionation in surface ultramafic environments (Albania). Earth and Planetary Science Letters, 423, 24–35.

Fujii T., Moynier F., Dauphas N. and Abe M. (2011)
Theoretical and experimental investigation of nickel isotopic fractionation in species relevant to modern and ancient oceans. Geochimica et Cosmochimica Acta, 75, 469–482.

Fraústo da Silva J.J.R. and Williams R.J.P. (2001)
The biological chemistry of the elements: The inorganic chemistry of life. Oxford University Press (Oxford), 600pp.

Gall L., Williams H.M., Siebert C., Halliday A.N., Herrington R.J. and Hein J.R. (2013)
Nickel isotopic compositions of ferromanganese crusts and the constancy of deep ocean inputs and continental weathering effects over the Cenozoic. Earth and Planetary Science Letters, 375, 148–155.

Gall L., Williams H., Siebert C. and Halliday A. (2012)
Determination of mass-dependent variations in nickel isotope compositions using double spiking and MC-ICP-MS. Journal of Analytical Atomic Spectrometry, 27, 137–145.

Gall L., Williams H.M., Halliday A.N. and Kerr A.C. (2017)
Nickel isotopic composition of the mantle. Geochimica et Cosmochimica Acta, 199, 196–209.

Gueguen B., Rouxel O., Ponzevera E., Bekker A. and Fouquet Y. (2013)
Nickel isotope variations in terrestrial silicate rocks and geological reference materials measured by MC-ICP-MS. Geostandards and Geoanalytical Research, 37, 297–317.

Gueguen B., Rouxel O., Rouget M.L., Bollinger C., Ponzevera E., Germain Y. and Fouquet Y. (2016)
Comparative geochemistry of four ferromanganese crusts from the Pacific Ocean and significance for the use of Ni isotopes as paleoceanographic tracers. Geochimica et Cosmochimica Acta, 189, 214–235.

Gueguen B., Sorensen J.V., Lalonde S.V., Peña J., Toner B.M. and Rouxel O. (2018)
Variable Ni isotope fractionation between Fe-oxyhydroxides and implications for the use of Ni isotopes as geochemical tracers. Chemical Geology, 481, 38–52.

Hatch J.R. and Leventhal J.S. (1992)
Relationship between inferred redox potential of the depositional environment and geochemistry of the Upper Pennsylvanian (Missourian) Stark Shale Member of the Dennis Limestone, Wabaunsee County, Kansas, USA. Chemical Geology, 99, 65–82.

Hogan M.E., Swift I.E. and Done J. (1983)
Urease assay and ammonia release from leaf tissues. Phytochemistry, 22, 663–667.

Javoy M., Kaminski E., Guyot F., Andrault D., Sanloup C., Moreira M. and Jaupart C. (2010)
The chemical composition of the Earth: Enstatite-chondrite models. Earth and Planetary Science Letters, 293, 259–268.

Jochum K.P., Nohl U., Herwig K., Lammel E., Stoll B. and Hofmann A.W. (2005)
GeoReM: A new geochemical database for reference materials and isotopic standards. Geostandards and Geoanalytical Research, 29, 333–338.

Jones B. and Manning D.A. (1994)
Comparison of geochemical indices used for the interpretation of palaeoredox conditions in ancient mudstones. Chemical Geology, 111, 111–129.

references

Konhauser K.O., Pecoits E., Lalonde S.V., Papineau D., Nisbet E.G., Barley M.E. and Kamber B.S. (2009)
Oceanic nickel depletion and a methanogen famine before the Great Oxidation Event. Nature, 458, 750.

Meija J., Coplen T.B., Berglund M., Brand W.A., De Bièvre P., Gröning M. and Prohaska T. (2016)
Isotopic compositions of the elements 2013 (IUPAC technical Report). Pure and Applied Chemistry, 88, 293–306.

Mudd G.M. (2010)
Global trends and environmental issues in nickel mining: Sulfides versus laterites. Ore Geology Reviews, 38, 9–26.

Nanne J.A., Nimmo F., Cuzzi J.N. and Kleine T. (2019)
Origin of the non-carbonaceous–carbonaceous meteorite dichotomy. Earth and Planetary Science Letters, 511, 44–54.

Okai T., Suzuki A., Kawahata H., Terashima S. and Imai N. (2002)
Preparation of a new Geological Survey of Japan geochemical reference material: Coral JCp-1. Geostandards Newsletter: The Journal of Geostandards and Geoanalysis, 26, 95–99.

Pašava J., Chrastný V., Loukola-Ruskeeniemi K. and Šebek O. (2018)
Nickel isotopic variation in black shales from Bohemia, China, Canada, and Finland: A reconnaissance study. Mineralium Deposita, 54, 1–24.

Porter S.J., Selby D. and Cameron V. (2014)
Characterising the nickel isotopic composition of organic-rich marine sediments. Chemical Geology, 387, 12–21.

Ragsale S.W. (2007)
Nickel and the carbon cycle. Journal of Inorganic Biochemistry, 101, 1657–1666.

Ratié G., Jouvin D., Garnier J., Rouxel O., Miska S., Guimarães E. and Thil F. (2015)
Nickel isotope fractionation during tropical weathering of ultramafic rocks. Chemical Geology, 402, 68–76.

Ratié G., Quantin C., Jouvin D., Calmels D., Ettler V., Sivry Y. and Garnier J. (2016)
Nickel isotope fractionation during laterite Ni ore smelting and refining: Implications for tracing the sources of Ni in smelter-affected soils. Applied Geochemistry, 64, 136–145.

Render J., Brennecka G.A., Wang S.J., Wasylenki L.E. and Kleine T. (2018)
A distinct nucleosynthetic heritage for early solar system solids recorded by Ni isotope signatures. The Astrophysical Journal, 862, 26.

Roelandts I. (1989)
Geological reference materials. Spectrochimica Acta Part B, 44, 5–29.

Rudnick R.L. and Gao S. (2003)
Composition of the continental crust. Treatise on Geochemistry, 3, 659.

Rugel G., Faestermann T., Knie K., Korschinek G., Poutivtsev M., Schumann D. and Wohlmuther M. (2009)
New measurement of the ^{60}Fe half-life. Physical Review Letters, 103, 072502.

Schovsbo N.H. (2001)
Why barren intervals? A taphonomic case study of the Scandinavian Alum Shale and its faunas. Lethaia, 34, 271–285.

Shi Z. (1994)
Nickel carbonyl: Toxicity and human health. Science of the Total Environment, 148, 293–298.

Šillerová H., Chrastný V., Vítková M., Francová A., Jehlička J., Gutsch M.R. and Jensen H.K. (2017)
Stable isotope tracing of Ni and Cu pollution in north-east Norway: Potentials and drawbacks. Environmental Pollution, 228, 149–157.

Spivak-Birndorf L.J., Wang S.J., Bish D.L. and Wasylenki L.E. (2018)
Nickel isotope fractionation during continental weathering. Chemical Geology, 476, 316–326.

Steele R.C., Elliott T., Coath C.D. and Regelous M. (2011)
Confirmation of mass-independent Ni isotopic variability in iron meteorites. Geochimica et Cosmochimica Acta, 75, 7906–7925.

Steele R.C., Coath C.D., Regelous M., Russell S. and Elliott T. (2012)
Neutron-poor nickel isotope anomalies in meteorites. The Astrophysical Journal, 758, 59.

Tang H. and Dauphas N. (2012)
Abundance, distribution, and origin of ^{60}Fe in the solar protoplanetary disk. Earth and Planetary Science Letters, 359, 248–263.

Ventura G.T., Gall L., Siebert C., Prytulak J., Szatmari P., Hürlimann M. and Halliday A.N. (2015)
The stable isotope composition of vanadium, nickel, and molybdenum in crude oils. Applied Geochemistry, 59, 104–117.

Wang S.J. and Wasylenki L.E. (2017)
Experimental constraints on reconstruction of Archaean seawater Ni isotopic composition from banded iron formations. Geochimica et Cosmochimica Acta, 206, 137–150.

Wang S.J., Rudnick R.L., Gaschnig R.M., Wang H. and Wasylenki L.E. (2019)
Methanogenesis sustained by sulfide weathering during the Great Oxidation Event. Nature Geoscience, 12, 296–300.

Wasylenki L.E., Howe H.D., Spivak-Birndorf L.J. and Bish D.L. (2015)
Ni isotope fractionation during sorption to ferrihydrite: Implications for Ni in banded iron formations. Chemical Geology, 400, 56–64.

Wasylenki L.E., Wells R.M. and Spivak-Birndorf L.J. (2014)
Ni sorption to birnessite drives a surprisingly large fractionation. In: AGU Fall Meeting Abstracts.

references

Watt R.K. and Ludden P.W. (1999)
Nickel-binding proteins. Cellular and Molecular Life Sciences (CMLS), 56, 604–625.

Wu G., Zhu J.M., Wang X., Han G., Tan D. and Wang S. (2019)
A novel purification method for high precision measurement of Ni isotopes by double spike MC-ICP-MS. Journal of Analytical Atomic Spectrometry, 34, 1639–1651.

Zhu J.M., Wu G., Wang X., Han G. and Zhang L. (2018)
An improved method of Cr purification for high precision measurement of Cr isotopes by double spike MC-ICP-MS. Journal of Analytical Atomic Spectrometry, 33, 809–821.

Supporting information

The following supporting information may be found in the online version of this article:

Figure S1. Comparison of data obtained with ESA and OPZ.

This material is available from: http://onlinelibrary.wiley.com/doi/10.1111/ggr.12321/abstract (This link will take you to the article abstract).